

# Self-assembly of a surfactin nanolayer at solid–liquid and air–liquid interfaces

Sagheer A. Onaizi<sup>1,2</sup> · M. S. Nasser<sup>3</sup> · Nasir M. A. Al-Lagtah<sup>1,2</sup>

Received: 21 September 2015 / Revised: 29 October 2015 / Accepted: 8 November 2015 / Published online: 9 December 2015  
© European Biophysical Societies' Association 2015

**Abstract** Surfactin, a sustainable and environmentally friendly surface active agent, is used as a model to study the adsorption of biosurfactants at hydrophobic and hydrophilic solid–liquid interfaces as well as the air–liquid interface. Surfactin adsorption was monitored as a function of time and concentration using surface plasmon resonance (SPR) technique in the case of the solid–liquid interfaces or the drop shape analysis (DSA) technique in the case of the air–liquid interface. The results obtained in this study showed that surfactin adsorption at the “hard” hydrophobic (functionalized with octadecanethiol) solid–liquid and the “soft” air–liquid interface were  $1.12 \pm 0.01 \text{ mg m}^{-2}$  (area per molecule of  $157 \pm 2 \text{ \AA}^2$ ) and  $1.11 \pm 0.05 \text{ mg m}^{-2}$  (area per molecule of  $159 \pm 7 \text{ \AA}^2$ ), respectively, demonstrating the negligible effect of the interface “hardness” on surfactin adsorption. The adsorption of surfactin at the hydrophilic (functionalized with  $\beta$ -mercaptoethanol) solid–liquid interface was about threefold lower than its adsorption at the hydrophobic–liquid interfaces, revealing the importance of hydrophobic interaction in surfactin adsorption process. The affinity constant of surfactin for the investigated interfaces follows the following order: air > octadecanethiol >  $\beta$ -mercaptoethanol. Biosurfactants, such as surfactin, are expected to replace the conventional fossil-based

surfactants in several applications, and therefore the current study is a contribution towards the fundamental understanding of biosurfactant behavior, on a molecular level, at hydrophobic and hydrophilic solid–liquid interfaces in addition to the air–liquid interface. Such understanding might aid further optimization of the utilization of surfactin in a number of industrial applications such as enhanced oil recovery, bioremediation, and detergency.

**Keywords** Surfactin · Adsorption · Hydrophobic · Hydrophilic · Surface plasmon resonance (SPR) · Surface tension

## Introduction

Human activities have caused several irreversible negative impacts on the environment. Air, soil, and water pollution, global warming, and the damage to ecological systems are some examples of the environmental footprints caused by several industries and their related applications. These alarming environmental issues have thus triggered the search for sustainable and more environmentally friendly technologies and products in order to replace several unclean and unsustainable ones. For example, more clean and sustainable surface active agents (i.e., biosurfactants) have emerged as replacers for synthetic surfactants, which are non-biodegradable and toxic in many cases, in addition to the fact that they are derived from polluting and unsustainable sources (i.e., fossil fuels). Among the known biosurfactants, surfactin is perhaps the most promising and powerful one. Although the discovery of surfactin traces back to 1968 when Arima et al. (1968) observed some biological and surface activity of this compound, its surface activity, particularly its assembly at solid–liquid interfaces,

✉ Sagheer A. Onaizi  
sagheer.onaizi@ncl.ac.uk; sagheer.onaizi@newcastle.ac.uk

<sup>1</sup> School of Chemical Engineering and Advanced Materials, Newcastle University, 537 Clementi Road, #06-01, Singapore 599493, Singapore

<sup>2</sup> School of Chemical Engineering and Advanced Materials, Newcastle University, Newcastle upon Tyne NE1 7RU, UK

<sup>3</sup> Gas Processing Center, College of Engineering, Qatar University, PO Box 2713, Doha, Qatar

is still not well documented in the literature. Surfactin is formed from a lactone ring containing seven amino acid residues (L-Glu  $\rightarrow$  L-Leu  $\rightarrow$  D-Leu  $\rightarrow$  L-Val  $\rightarrow$  L-Asp  $\rightarrow$  D-Leu  $\rightarrow$  L-Leu) (Kakinuma et al. 1969), linked to a  $\beta$ -fatty acid (lipidic) via a lactone bond (Lu et al. 2007; Onaizi et al. 2014a; Peypoux et al. 1999).

Several studies have related the exceptional and the wide performance of surfactin to its structure. The interfacial activity of surfactin arises from its amino acid characteristics and sequence (Mulligan 2005). Surfactin has an amphiphilic character; the two amino acids (Glu and Asp) provide the hydrophilic domain, while the other amino acids and the fatty acid chain provide the hydrophobic moiety (Bonmatin et al. 1994; Gallet et al. 1999; Lu et al. 2007). This nature promotes surfactin folding into a  $\beta$ -sheet structure, resembling a horse saddle (Gallet et al. 1999; Ishigami et al. 1995; Lu et al. 2007), which explains its wide biological and interfacial activity (Bonmatin et al. 1994; Peypoux et al. 1999). For example, surfactin can reduce the interfacial tension of the water–air and water–hexadecane systems from 72.8 to 27.9 mN m<sup>-1</sup> (Arima et al. 1968; Cooper et al. 1981) and from 40 to 1 mN m<sup>-1</sup> (Cooper et al. 1981), respectively. Additionally, the molar fractions of surfactin in the mixed surfactin–sodium dodecylbenzenesulphonate monolayer at the air–liquid interface and also in the mixed micelle were more than five times greater than its fraction in the monomeric binary liquid mixture (Onaizi et al. 2012). Furthermore, a detergent formulation containing surfactin has shown a superior cleaning performance of protein stains from solid surfaces relative to those containing synthetic surfactants (Onaizi et al. 2009b). Such powerful interfacial and wetting characteristics are key requirements in a number of industrial applications such as enhanced oil recovery, detergency, and foams and emulsions. Surfactin has also a potential to be used in the remediation of soil and water contaminated with heavy metals, which is a serious issue in several industries, since it forms complexes with metal ions due to its negatively charged Glu and Asp amino acids (Bonmatin et al. 1994; Thimon et al. 1992).

The attractiveness of biosurfactants (such as surfactin) as potential replacers for synthetic surfactants in many industrial applications (in addition to their potential unique applications) is obvious. These applications mainly depend on the amphiphilic nature of the biosurfactant molecules. Therefore, the usage of biosurfactants in many applications (detergents, emulsions, enhanced oil recovery, etc.) will not be optimized without understanding their interfacial behaviors. Hence, the main aim of the current study is to reveal the self-assembling tendency of a model biosurfactant (surfactin) at solid–liquid interfaces with hydrophobic and hydrophilic characteristics. The fundamental analysis of the assembly process in terms of adsorption

isotherm and parameters will also be carried out. Additionally, the assembly of surfactin at the air–liquid interface will be studied using surface tension measurements; the data obtained from these measurements will be mathematically analyzed in order to predict the adsorption parameters of surfactin at the air–liquid interface, allowing for quantitative comparison with surfactin adsorption at the solid–liquid interfaces. The findings reported in this study reveal some useful information on the packing density and also the affinity of surfactin for the different interfaces, which might be useful in designing products containing surfactin to be used in some industrial applications (e.g., detergent formulations and foams and emulsions).

## Materials and methods

Surfactin was purchased from Wako Pure Chemical Industries Ltd (Japan). Surface plasmon resonance (SPR) spectroscopy (Resonant Probes GmbH, Göttingen, Germany) was used in this study to monitor the adsorption of surfactin at the hydrophobic and hydrophilic solid–liquid interfaces, while a Krüss drop shape analysis system DSA10 (Krüss GmbH, Hamburg, Germany) was used to measure the changes in the air–liquid interfacial tension induced by surfactin adsorption. SPR sensor chips (SF10 glass slides, 25  $\times$  25 mm, coated with  $\sim$ 45 nm gold film) were purchased from Nanofilm Technologie GmbH (Germany). These sensor chips were functionalized to display hydrophobic or hydrophilic characteristics using the self-assembly (Onaizi and Leong 2011) of octadecanethiol (purchased from Sigma) and  $\beta$ -mercaptoethanol (purchased from Merck) monolayers, respectively, according to the previously published protocol (Onaizi et al. 2009a, b). Before the assembly process, the chips were thoroughly cleaned by extensive wash with Milli-Q water (MQW) and then with 10 % (v/v) Decon 90 aqueous solution. The detergent solution was heated up slowly until the temperature reached 70 °C, and then the solution was discarded and the chips were rinsed several times with MQW. After this, the chips were rinsed with HPLC-grade ethanol, followed by rinsing with MQW again. The chips were then placed in 5:1:1 (v/v) mixture of MQW: H<sub>2</sub>O<sub>2</sub> (30 % v/v solution): NH<sub>4</sub>OH (30 % v/v solution) and the solution was kept at 70–80 °C for at least 20 min (practically until no gas bubbles appeared from the surfaces of the chips). Following this, the chips were washed with MQW and HPLC-grade ethanol. Finally, the chips were immersed in 1 mg ml<sup>-1</sup> ethanolic solution of octadecanethiol (ODT) or  $\beta$ -mercaptoethanol (BME) at room temperature for at least 1 day.

To study the adsorption of surfactin on the functionalized biosensor chips, the SPR flow cell mounted with the

chip of interest was equilibrated with 20 mM sodium phosphate buffer (pH 8) prior to the injection of surfactin solution (in the same buffer). The progress of surfactin adsorption as a function of time was followed by SPR. Once the equilibrium was attained, the bulk concentration of surfactin was increased, leading to another equilibrium data point. The equilibrium data points were used to establish the experimental isotherms of surfactin at the solid–liquid interfaces; these experimental isotherms were regressed using the Langmuir adsorption isotherms, allowing the prediction of the maximum adsorption density of surfactin ( $\Gamma_{\max}$ ) as well as the affinity constant ( $K_a$ ).

The adsorption of surfactin at the air–liquid interface was obtained from the surface tension measurements, which were performed using the DSA10 instrument. At the beginning of every surface tension experiment, 8 ml of surfactin solution (in 20 mM sodium phosphate buffer, pH 8) at a given concentration was placed in an acid-cleaned quartz cuvette and then  $\sim 8 \mu\text{l}$  of pendant air bubble was created in the solution. The dynamic surface tension was then monitored continuously until equilibrium was established. At least duplicate runs at each surfactin concentration were performed to confirm reproducibility; the variations in the equilibrium surface tension from one run to another never exceeded 3 %. The equilibrium surface tension–surfactin concentration data were used to predict the parameters of surfactin adsorption at the air–liquid interface as described in the following “Results and discussion” section.

## Results and discussion

Surfactin adsorption at the solid–liquid interfaces was monitored using SPR. The shift in the SPR angle following surfactin adsorption was converted into an average film thickness using Winspall software (v 2.20, MPI-für Polymerforschung, Mainz, Germany) simulations, which are based on Fresnel equations and Kretschmann configuration (Damos et al. 2005; de Bruijn et al. 1991, 1993; Oudshoorn et al. 1996; Peterlinz and Georgiadis 1996). In these simulations, the refractive index of surfactin was set at 1.462 (<http://www.chemnet.com/cas/en/24730-31-2/surfactin-from-bacillus-subtilis.html>). The average equilibrium thicknesses of the adsorbed films at the corresponding bulk concentrations of surfactin were converted to average mass per unit area of the interface ( $\text{mg m}^{-2}$ ) using the density of surfactin, which is  $1.037 \text{ g cm}^{-3}$  (<http://www.chemnet.com/cas/en/24730-31-2/surfactin-from-bacillus-subtilis.html>). These surface coverage–surfactin bulk concentration data points were used to establish the experimental adsorption isotherms. The adsorption parameters of surfactin at the hydrophobic ODT–liquid and the hydrophilic BME–liquid interfaces were obtained from the regression of the

experimental data. Owing to its simplicity, the Langmuir adsorption isotherm is widely used to predict the adsorption behavior of several components at solid–liquid interfaces, including biomolecules (Onaizi et al. 2009a, 2010; Roach et al. 2005; Scopelliti et al. 2010). Thus, it will be used in this study. Although the underlying assumptions of the Langmuir adsorption isotherm might not be fully met (in particular the assumption of reversible adsorption and negligible interactions between adsorbed molecules), it has been reported that it tracks the adsorption data of surface active agents (including biomolecules) at fluid–fluid and solid–fluid interfaces reasonably well (Delgado et al. 2006; Giribabu and Ghosh 2007; Lin et al. 2002; Onaizi et al. 2009a, 2010, 2014a, b, 2015). The Langmuir adsorption isotherm relates the surface coverage to the bulk concentration of the solute as follows:

$$\Gamma = \frac{K_a \Gamma_{\max} C}{1 + K_a C} \quad (1)$$

where  $\Gamma$ ,  $\Gamma_{\max}$ ,  $C$ , and  $K_a$  are the surface coverage (concentration) of the adsorbed surfactin, the maximum adsorption density, the concentration of surfactin in bulk and the affinity constant (i.e., the ratio of adsorption to desorption rate constants), respectively.

## Surfactin adsorption at the hydrophilic solid–liquid interface

The BME surface is terminated with the hydroxyl group (see Fig. 1). Additionally, BME contact angle with MQW is  $31^\circ$  (Onaizi et al. 2010). Thus, the BME surface is an uncharged (neutral) hydrophilic surface. On the other hand, the pKa values of Asp and Glu (the two ionizable amino acids of surfactin) are 4.3 and 4.5, respectively (Zou et al. 2010). Accordingly, surfactin is fully ionized at pH 8 (Carrillo et al. 2003; Li et al. 2013; Zou et al. 2010), making surfactin molecules negatively charged ions under the experimental conditions of this study. Therefore, the mode of interaction between surfactin and the BME surface is expected to be mainly through hydrogen bonding and van der Waals forces. Figure 2 shows the adsorption of surfactin onto the BME surface. Although the adsorption is not strong, surfactin still accumulates onto the BME surface to certain extents. This observation is different from that reported by Shen et al. (2011) in which surfactin did not adsorb on the hydrophilic sapphire surface when the pH of the adsorption medium was close to the isoelectric point of sapphire (i.e., when the surface was neutral). However, anionic synthetic surfactants have been reported to adsorb on uncharged hydrophilic surfaces (including BME) to certain extents (Onaizi et al. 2015; Tiberg et al. 2000), which is in line with the finding of the current study.

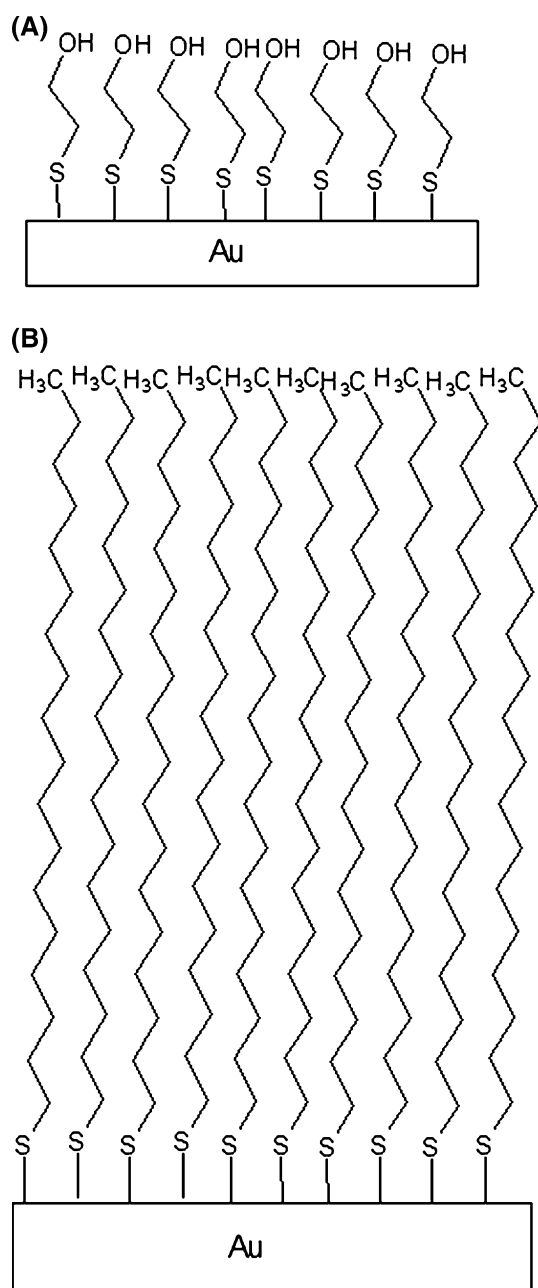


**Fig. 1** Idealized structures (not drawn to scale or exact orientations) of the functionalized SPR chips showing the self-assembled monolayer (SAM) of **a**  $\beta$ -mercaptoethanol (BME) and **b** octadecanethiol (ODT)

The experimental data shown in Fig. 2 were regressed using the Langmuir adsorption isotherm (see Fig. 2). The regression provided two important quantities, the maximum adsorption density ( $\Gamma_{\max}$ ) and the affinity constant ( $K_a$ ). The predicted values of  $\Gamma_{\max}$  and  $K_a$  are  $0.44 \pm 0.03 \text{ mg m}^{-2}$  and  $(1.6 \pm 0.3) \times 10^5 \text{ M}^{-1}$ , respectively. Thus, the area occupied by a surfactin molecule at the BME–liquid interface is  $401 \pm 27 \text{ \AA}^2$ , which is quite high (almost threefold

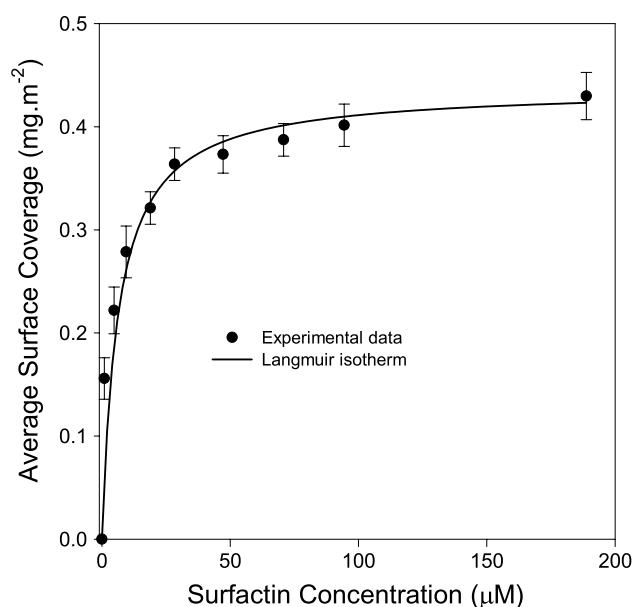


**Fig. 2** Non-linear regression of the equilibrium surface coverage of surfactin at the hydrophilic (BME) solid–liquid interface as a function of its bulk concentration using Eq. (1). The adsorption took place from 20 mM sodium phosphate buffer at pH 8. The predicted maximum adsorption density and affinity constant are  $0.44 \pm 0.03 \text{ mg m}^{-2}$  and  $(1.6 \pm 0.3) \times 10^5 \text{ M}^{-1}$ , respectively

higher than the area occupied by the surfactin molecule at the hydrophobic ODT–liquid interface, see the subsequent section). The likely possible reason(s) for such high molecular area is (are): (i) surfactin molecules widely spread on the BME surface or/and (ii) the surface is not fully covered by the adsorbed surfactin molecules. It has been reported that surfactin adopts a ball-like structure under similar experimental conditions (Shen et al. 2011). The wide spread of surfactin molecules on the BME surface would require a strong interaction between the surface and surfactin to open up and flatten such a structure. Although it has been reported that surfactin interacted hydrophobically, to a certain extent, with a hydrophilic surface (sapphire) (Shen et al. 2011), it is unlikely for the hydrophobic (if any) surfactin–BME interaction to be stronger than the hydrophobic surfactin–ODT interaction given that ODT is more hydrophobic than BME. Thus, hydrophobic interaction between the BME surface and surfactin is unlikely to be significant. Additionally, Coulombic attraction is also absent since the BME surface is neutral (uncharged). Thus, a wide spread of surfactin molecules on the BME surface is unlikely to be the cause of this high molecular area of surfactin at the BME–liquid interface. Therefore, it seems reasonable to assume that surfactin does not fully cover the BME surface and there are some surfactin-free “islands” on the BME surface. This assumption is supported by the likelihood that water molecules could also interact with the

hydrophilic (OH-terminated) BME surface through hydrogen bonding; such BME–water interaction could reduce the available binding sites, leading to surfactin-free patches on the surface. Such scenario was also proposed for an anionic synthetic surfactant adsorption at the BME–liquid interface (Onaizi et al. 2015). Another support for the aforementioned assumption is the finding reported by Shen et al. (2011) where surfactin did not fully cover the hydrophilic sapphire surface even when the surface is slightly positively charged. It must be highlighted in this context that the non-uniformity (if any) of the adsorbed films does not compromise the validity/accuracy of the obtained results since the sensing of the SPR instrument used in this study is based on the mass of the material bound to the surface and not on the thickness uniformity of the adsorbed film.

### Surfactin adsorption at the hydrophobic solid–liquid interface

ODT is an uncharged hydrophobic surface [contact angle with MQW is  $93^\circ$  (Onaizi et al. 2010)]. Thus, ODT–surfactin interaction is expected to be mainly hydrophobically driven. The adsorption of surfactin at the ODT–liquid interface is shown in Fig. 3. The experimental data points were fitted using the Langmuir adsorption isotherm to provide estimates for  $\Gamma_{\max}$  and  $K_a$ . The predicted  $\Gamma_{\max}$  is

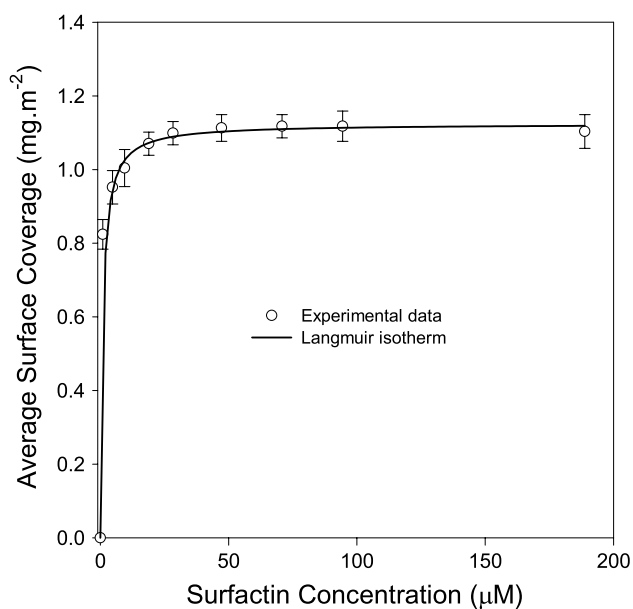


**Fig. 3** Non-linear regression of the equilibrium surface coverage of surfactin at the hydrophobic (ODT) solid–liquid interface as a function of its bulk concentration using Eq. (1). The adsorption took place from 20 mM sodium phosphate buffer at pH 8. The predicted maximum adsorption density and affinity constant are  $1.12 \pm 0.01 \text{ mg m}^{-2}$  and  $(1.1 \pm 0.1) \times 10^6 \text{ M}^{-1}$ , respectively

$1.12 \pm 0.01 \text{ mg m}^{-2}$ , corresponding to an area per surfactin molecule at the ODT–liquid interface of  $157 \pm 2 \text{ \AA}^2$ . This value is close to that ( $145 \pm 5 \text{ \AA}^2$ ) reported by Shen et al. (2009) for surfactin adsorption on octadecyltrichlorosilane-coated silicon (a hydrophobic surface) using neutron reflectivity. The slightly lower surface area per molecule reported by Shen et al. (2009) is probably due to the higher hydrophobicity of octadecyltrichlorosilane [contact angle with MQW is about  $112^\circ$  (Ren et al. 2002)]. This higher hydrophobicity might have led to a more dense packing of surfactin molecules, resulting in a lower surface area per surfactin molecule at the octadecyltrichlorosilane–liquid interface.

The area occupied by a surfactin molecule at the hydrophobic ODT–liquid interface is about one-third of its molecular area at the hydrophilic BME–liquid interface, highlighting the higher packing of surfactin molecules at the hydrophobic ODT–liquid relative to the hydrophilic BME–liquid interface. This finding contradicts the observations reported by Hajfarajollah et al. (2015) and Meylheuc et al. (2006), where higher biosurfactant adsorption on hydrophilic surfaces was obtained. However, the hydrophilic surfaces utilized by these researchers carried a permanent opposite charge to that on the investigated biosurfactant, resulting in a strong Coulombic attraction between the given surface and the biosurfactant molecules. This is not the case for the uncharged BME surface, with which surfactin interacts via relatively weak van der Waals and hydrogen bonding. Thus, it is not surprising that surfactin adsorbs less onto BME compared to ODT surface. Higher adsorption (almost threefold) on ODT relative to BME surface was also reported for the anionic sodium dodecylbenzenesulphonate surfactant (Onaizi et al. 2015). Other synthetic surfactants have also been reported to adsorb more on hydrophobic than on uncharged hydrophilic surfaces (Tiberg et al. 2000). Thus, there is a clear evidence that when the Coulombic attractive or hydrophobic interactions are absent, (bio)-surfactant molecules adsorb in a less compact manner.

In addition to the higher packing density at the ODT–liquid relative to the BME–liquid interface, surfactin has also higher affinity for the ODT surface. The estimated affinity ( $K_a$ ) for the ODT–liquid interface is  $(1.1 \pm 0.1) \times 10^6 \text{ M}^{-1}$ , which is one order of magnitude higher than its affinity for the BME–liquid interface. Higher affinity usually results from strong interactions between adsorbent and adsorbate (Onaizi et al. 2014b). It has been assumed in the previous section that surfactin interacts much more strongly with the hydrophobic ODT surface than with the hydrophilic uncharged BME surface. The higher affinity of surfactin for the ODT surface strongly supports this assumption. This finding, along with the higher packing of surfactin molecules at the ODT–liquid interface, demonstrates the



hydrophobicity effect on surfactin adsorption at uncharged solid–liquid interfaces.

### Surfactin adsorption at the air–liquid interface

As shown in Fig. 3, the maximum adsorption was achieved at about 47- $\mu\text{M}$  bulk concentration of surfactin. Above this concentration, there was a negligible change in the surface coverage of surfactin with a further increase in its concentration in bulk. Owing to the amphiphilic nature of surface active agents, such as surfactin, these agents tend to assemble at hydrophobic–hydrophilic interfaces (He et al. 2009, 2011; Onaizi et al. 2007), thus minimizing their free energy. However, due to coverage limitations, saturation in adsorption is reached, above which there is a negligible increase in the (bio)-surfactant population at the interface. Such a phenomenon is usually accompanied by the formation of micelles in the solution to minimize the hydration of the hydrophobic portion of the (bio)-surfactant molecules. It has been observed in some studies that the saturation condition was attained at the critical micelle concentration (CMC) of the surfactants (Király et al. 1997; Levitz 2002; Lindheimer et al. 1990; Partyka et al. 1984). The question is, therefore, whether 47  $\mu\text{M}$  is equivalent to the CMC of surfactin in 20 mM phosphate buffer, pH 8, or not. In other words, does the plateau in surfactin adsorption at the solid–liquid interfaces correspond to the surfactin CMC? To answer this question, surface tension measurements of an air bubble in different concentrations of surfactin were performed and the result is shown in Fig. 4. It is clear that the surface tension levels off at surfactin concentration of  $\sim 47 \mu\text{M}$  (see also the inset in Fig. 4), suggesting that this value is the CMC of surfactin in 20 mM sodium phosphate buffer at pH 8. Thus, the start of the plateau of surfactin adsorption at the ODT–liquid interface is matching the onset of micellization. However, for surfactin adsorption at the BME–liquid interface, there is still little increase (even though insignificant) in surfactin adsorption beyond the CMC, probably due to the low packing density of surfactin molecules at the BME–liquid interface. Such a trend has also been reported for other surfactant adsorption at solid–liquid interfaces (Paria and Khilar 2004; Rojas et al. 2002).

To compare surfactin adsorption at the air–liquid interface to its adsorption at the hydrophobic and hydrophilic solid–liquid interfaces, the surface tension data were mathematically analyzed. Starting from the Gibbs equation of state coupled with the Langmuir adsorption isotherm, the following equation was derived:

$$\gamma^e = \gamma_0 - RT\Gamma_{\max} \ln(1 + K_a C) \quad (2)$$

where  $\gamma^e$  is the equilibrium surface tension at a given surfactin concentration,  $\gamma_0$  ( $\approx 72.8 \text{ mN m}^{-1}$ ) is the surface

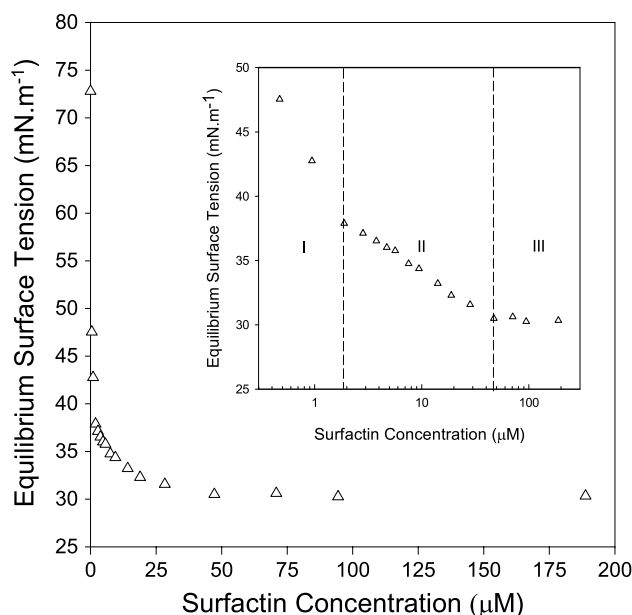


**Fig. 4** The equilibrium tension of the air–liquid interface as a result of surfactin adsorption, which took place from different surfactin solutions in 20 mM sodium phosphate buffer, pH 8. The *inset* is the plot of the equilibrium tension of the air–liquid interface as a function of the logarithm of surfactin concentration. The change in the equilibrium surface tension with surfactin concentration is high in region I before slowing down in region II and finally reaching a steady value in region III. The intersection of regions II and III represents the CMC ( $\sim 47 \mu\text{M}$ ) of surfactin in 20 mM sodium phosphate buffer, pH 8

tension of surfactin-free liquid,  $R$  is the universal gas constant and  $T$  is the absolute temperature.

The above equation is only applicable up to the CMC of the surface active agent. The regression of the  $\gamma^e - C$  data in the pre-micellar region using Eq. (2) provided unsatisfactory fitting (results not shown). To get insight into the possible reason(s) for such unsatisfactory fitting, the  $\gamma^e - \ln C$  data were plotted as shown in the inset of Fig. 4. The  $\gamma^e - \ln C$  plot has two distinct slopes in the pre-micellar region, which could be the reason for the low-quality fitting of the whole pre-micellar  $\gamma^e - C$  data using Eq. (2). Therefore, the  $\gamma^e - C$  data in regions I and II (see the inset in Fig. 4) were regressed separately. The  $\gamma^e - C$  data in region I were fitted using Eq. (2) while those in region II were fitted using the following equation after taking the new boundary conditions into account:

$$\gamma_{\text{II}}^e = \gamma_{\text{I-II}} - RT\Gamma_{\max} \ln \left( \frac{1 + K_a C_{\text{II}}}{1 + K_a C_{\text{I-II}}} \right) \quad (3)$$

where  $\gamma_{\text{II}}^e$ , and  $C_{\text{II}}$  are, respectively, the equilibrium surface tension and surfactin concentration in region II;  $\gamma_{\text{I-II}}$  and  $C_{\text{I-II}}$  are, respectively, the surface tension and surfactin concentration at the intersection of I and II regions.

The fitting of  $\gamma^e - C$  data in region I (results not shown) gave an estimate of  $58 \pm 1 \text{ \AA}^2$  for the area occupied by a surfactin molecule at the air–liquid interface. Maget-Dana and Ptak (1992) reported a smaller value ( $32 \text{ \AA}^2$ ) for surfactin molecular area at the air–liquid interface. However, this area is quite small and physically unlikely for a relatively large surfactin molecule (Li et al. 2013). It is even smaller than the molecular areas of several low molecular weight surfactants. It has been reported that at low surfactin concentrations, such as those in region I, the strong adsorption of surfactin to the air–liquid interface leads to the depletion of surfactin molecules in the bulk solution, resulting in a steep slope of  $\gamma^e - \ln C$ , which in turn gives an inaccurately low surface area per surfactin molecule (Li et al. 2013). Therefore,  $\gamma^e - C$  data in region I were excluded and only those in region II were used to predict the maximum adsorption density of surfactin at the air–liquid interface and also its affinity for the interface using Eq. (3). The fitting of  $\gamma^e - C$  in region II is shown in Fig. 5. The estimated maximum adsorption density ( $\Gamma_{\max}$ ) of surfactin at the air–liquid interface is  $1.11 \pm 0.05 \text{ mg m}^{-2}$ , which corresponds to an area per molecule of  $159 \pm 7 \text{ \AA}^2$ . This area is close to that ( $147 \pm 5 \text{ \AA}^2$ ) predicted by Li et al. (2013) using neutron reflectivity. Jang and Goddard III (2006) also reported a comparable ( $170 \text{ \AA}^2$ ) molecular area for a surfactin monolayer film using molecular dynamic simulations.

Strikingly, the molecular area of surfactin at the air–liquid interface is close to its molecular area at the

ODT–liquid interface, which is  $157 \pm 2 \text{ \AA}^2$ . In both cases, the adsorption is mainly driven by hydrophobic interactions. Interestingly, the nature of the interface (soft or hard) seems to have a negligible effect on surfactin adsorption. The affinity of surfactin for the air–liquid interface was estimated to be  $(1.5 \pm 0.6) \times 10^6 \text{ M}^{-1}$ .

Comparing the affinity of surfactin for the three interfaces investigated in this work reveals that the affinity of surfactin for the hydrophilic solid–liquid interface is an order of magnitude lower than its affinity for the hydrophobic solid–liquid or the air–liquid interface. Furthermore, the affinity of surfactin for the “hard” hydrophobic solid–liquid interface is slightly lower than its affinity for the “soft” air–liquid interface.

## Conclusions

Surfactin self-assembly at the investigated interfaces is strongly affected by the hydrophobicity of the interface. The adsorption of surfactin at the two hydrophobic–hydrophilic (i.e., the ODT–liquid and the air–liquid) interfaces is about three times its adsorption at the hydrophilic–hydrophilic (i.e., the BME–liquid) interface. The maximum adsorption density of surfactin at the BME solid–surface interface is  $0.44 \pm 0.03 \text{ mg m}^{-2}$ , corresponding to an area per molecule of  $401 \pm 27 \text{ \AA}^2$ . This area is quite large, suggesting a wide spread of surfactin on the BME surface or/and the presence of unoccupied “islands” on the surface; the latter proposition is the most likely. One of the interesting findings reported in this work is the similar packing of surfactin (i.e., area per molecule) at the hydrophobic–hydrophilic interfaces whether the interface is hard (solid–liquid) or soft (air–liquid), demonstrating a negligible effect of the interface *hardness*. The results presented in this work provide fundamental insights into the self-assembly of surfactin at three different interfaces. A fundamental understanding of biosurfactants adsorption at interfaces will aid in optimizing the utilization of these renewable and environmentally friendly surface active agents in several industrial applications such as enhanced oil recovery, emulsions, cosmetics, and detergents.

## References

- Arima K, Kakinuma A, Tamura G (1968) Surfactin, a crystalline peptidolipid surfactant produced by *Bacillus subtilis*: isolation, characterization and its inhibition of fibrin clot formation. *Biochem Biophys Res Commun* 31:488–494
- Bonmatin J-M, Cenest M, Labbe H, Ptak M (1994) Solution three-dimensional structure of surfactin: a cyclic lipopeptide studied by  $^1\text{H}$ NMR, distance geometry, and molecular dynamics. *Biopolymers* 34:975–986

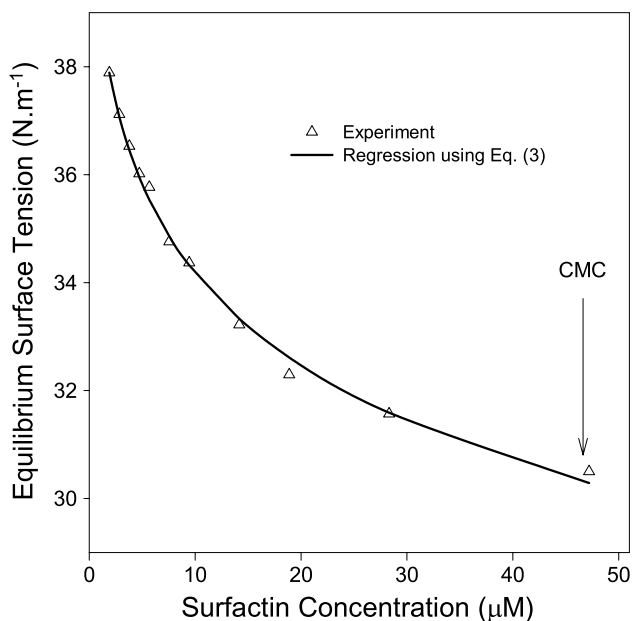


**Fig. 5** Non-linear regression of the equilibrium surface tension–surfactin concentration data in region II using Eq. (3). The predicted maximum adsorption density and affinity constant are  $1.11 \pm 0.05 \text{ mg m}^{-2}$  and  $(1.5 \pm 0.6) \times 10^6 \text{ M}^{-1}$ , respectively

- Carrillo C, Teruel JA, Aranda FJ, Ortiz A (2003) Molecular mechanism of membrane permeabilization by the peptide antibiotic surfactin. *Biochim Biophys Acta* 1611:91–97
- Cooper DG, Macdonald CR, Duff SJB, Kosaric N (1981) Enhanced production of surfactin from *Bacillus subtilis* by continuous product removal and metal cation additions. *Appl Environ Microbiol* 42:408–512
- Damos FS, Luz RCS, Kubota LT (2005) Determination of thickness, dielectric constant of thiol films, and kinetics of adsorption using surface plasmon resonance. *Langmuir* 21:602–609
- de Bruijn HE, Altenburg BSF, Kooyman RPH, Greve J (1991) Determination of thickness and dielectric constant of thin transparent dielectric layers using surface plasmon resonance. *Opt Commun* 82:425–432
- de Bruijn HE, Minor M, Kooyman RPH, Greve J (1993) Thickness and dielectric constant determination of thin dielectric layers. *Opt Commun* 95:183–188
- Delgado C, Merchan MD, Velazquez MM, Anaya J (2006) Effect of surfactant structure on the adsorption of carboxybetaines at the air–water interface. *Colloid Surf A* 280:17–22
- Gallet X, Deleu M, Razafindralambo H, Jacques P, Thonart P, Paquot M, Brasseur R (1999) Computer simulation of surfactin conformation at a hydrophobic/hydrophilic interface. *Langmuir* 15:2409–2413
- Giribabu K, Ghosh P (2007) Adsorption of nonionic surfactants at fluid–fluid interfaces: importance in the coalescence of bubbles and drops. *Chem Eng Sci* 62:3057–3067
- Hajfarajollah H, Mehvari S, Habibian M, Mokhtarani B, Noghabi KA (2015) Rhamnolipid biosurfactant adsorption on a plasma-treated polypropylene surface to induce antimicrobial and anti-adhesive properties. *RSC Adv* 5:33089–33097
- He L, Malcolm AS, Dimitrijević M, Onaizi SA, Shen H-H, Holt SA, Dexter AF, Thomas RK, Middelberg APJ (2009) Cooperative tuneable interactions between a designed peptide biosurfactant and positional isomers of SDOBS at the air–water interface. *Langmuir* 25:4021–4026
- He L, Onaizi SA, Dimitrijević M, Malcolm AS, Shen H-H, Dong C, Holt SA, Thomas RK, Middelberg APJ (2011) Comparison of positional surfactant isomers for displacement of rubisco protein from the air–water interface. *J Colloid Interface Sci* 360:617–622
- Ishigami Y, Osman M, Nakahara H, Sano Y, Ishiguro R, Matusumoto M (1995) Significance of  $\beta$ -sheet formation for micellization and surface adsorption on surfactin. *Colloids Surf B* 4:341–348
- Jang SS, Goddard WA III (2006) Structures and properties of Newton black films characterized using molecular dynamics simulations. *J Phys Chem B* 110:7992–8001
- Kakinuma A, Ouchida A, Shima T, Sugino H, Isono H, Tamura G, Arima K (1969) Confirmation of the structure of surfactin by mass spectrometry. *Agric Biol Chem* 33:1669–1671
- Kiraly Z, Borner RHK, Findenegg GH (1997) Adsorption and aggregation of  $C_8E_4$  and  $C_8G_1$  nonionic surfactants on hydrophilic silica studied by calorimetry. *Langmuir* 13:3308–3315
- Levitz PE (2002) Adsorption of non-ionic surfactants at the solid/water interface. *Colloids Surf A* 205:31–38
- Li PX, Li ZX, Shen H-H, Thomas RK, Penfold J, Lu JR (2013) Application of the Gibbs equation to the adsorption of nonionic surfactants and polymers at the air–water interface: comparison with surface excesses determined directly using neutron reflectivity. *Langmuir* 29:9324–9334
- Lin S-Y, Dong C, Hsu T-J, Hsu C-T (2002) Determination of adsorption of an ionic surfactant on latex from surface tension measurements. *Colloid Surf A* 196:189–198
- Lindheimer M, Keh E, Zaini S, Partyka S (1990) Interfacial aggregation of nonionic surfactants onto silica gel: calorimetric evidence. *J Colloid Interface Sci* 138:83–91
- Lu JR, Zhao XB, Yaseen M (2007) Biomimetic amphiphiles: biosurfactants. *Curr Opin Colloid Interface Sci* 12:60–67
- Maget-Dana R, Ptak M (1992) Interfacial properties of surfactin. *J Colloid Interface Sci* 153:285–291
- Meylheuc T, Renault M, Bellon-Fontaine MN (2006) Adsorption of a biosurfactant on surfaces to enhance the disinfection of surfaces contaminated with *Listeria monocytogenes*. *Int J Food Microbiol* 109:71–78
- Mulligan CN (2005) Environmental applications for biosurfactants. Environmental pollution. *Environ Pollut* 133:183–198
- Onaizi SA, Leong SSS (2011) Tethering antimicrobial peptides: current status and potential challenges. *Biotechnol Adv* 29:67–74
- Onaizi SA, Malcolm AS, He L, Middelberg APJ (2007) Directed disassembly of an interfacial rubisco protein network. *Langmuir* 23:6336–6341
- Onaizi SA, He L, Middelberg APJ (2009a) Proteolytic cleaning of a surface-bound rubisco protein stain. *Chem Eng Sci* 64:3868–3878
- Onaizi SA, He L, Middelberg APJ (2009b) Rapid screening of surfactant and biosurfactant surface cleaning performance. *Colloid Surf B* 72:68–74
- Onaizi SA, He L, Middelberg APJ (2010) The construction, fouling and enzymatic cleaning of a textile dye surface. *J Colloid Interface Sci* 351:203–209
- Onaizi SA, Nasser MS, Twaiq FA (2012) Micellization and interfacial behavior of a synthetic surfactant–biosurfactant mixture. *Colloid Surf A* 415:388–393
- Onaizi SA, Nasser MS, Twaiq FA (2014a) Adsorption and thermodynamics of biosurfactant, surfactin, monolayers at the air-buffered liquid interface. *Colloid Polym Sci* 292:1649–1656
- Onaizi SA, Nasser MS, Twaiq FA (2014b) Lysozyme binding to tethered bilayer lipid membranes prepared by rapid solvent exchange and vesicle fusion methods. *Eur Biophys J* 43:191–198
- Onaizi SA, Nasser MS, Al-Lagtah NMA (2015) Adsorption of an anionic surfactant at air–liquid and different solid–liquid interfaces from solutions containing high counter-ion concentration. *Colloid Polym Sci* 293:2891–2899
- Oudshoorn RGC, Kooyman RPH, Greve J (1996) Refractive index and layer thickness of an adsorbing protein as reporters of monolayer formation. *Thin Solid Films* 284–285:836–840
- Paria S, Khilar KC (2004) A review on experimental studies of surfactant adsorption at the hydrophilic solid–water interface. *Adv Colloid Interface Sci* 110:75–95
- Partyka S, Zaina S, Lindheimer M, Brun B (1984) The adsorption of non-ionic surfactants on a silica gel. *Colloid Surf* 12:255–270
- Peterlinz KA, Georgiadis R (1996) In situ kinetics of self-assembly by surface plasmon resonance spectroscopy. *Langmuir* 12:4731–4740
- Peypoux F, Bonmatin JM, Wallach J (1999) Recent trends in the biochemistry of surfactin. *Appl Microbiol Biotechnol* 51:553–563
- Ren S, Yang S, Zhao Y, Zhou J, Xu T, Liu W (2002) Friction and wear studies of octadecyltrichlorosilane SAM on silicon. *Tribol Lett* 13:233–239
- Roach P, Farrar D, Perry CC (2005) Interpretation of protein adsorption: surface-induced conformational changes. *J Am Chem Soc* 127:8168–8173
- Rojas OJ, Macakova L, Blomberg E, Emmer A, Claesson PM (2002) Fluorosurfactant self-assembly at solid/liquid interfaces. *Langmuir* 18:8085–8095
- Scopelliti PE, Borgonovo A, Indrieri M, Giorgetti L, Bongiorno G, Carbone R, Podesta A, Milani P (2010) The effect of surface nanometre-scale morphology on protein adsorption. *PLoS ONE* 5:e11862
- Shen H-H, Thomas RK, Chen C-Y, Darton RC, Baker SC, Penfold J (2009) Aggregation of the naturally occurring lipopeptide,



- surfactin, at interfaces and in solution: an unusual type of surfactant? *Langmuir* 25:4211–4218
- Shen H-H, Lin T-W, Thomas RT, Taylor DJF, Penfold J (2011) Surfactin structures at interfaces and in solution: the effect of pH and cations. *J Phys Chem B* 115:4427–4435
- Thimon L, Peypoux F, Michel G (1992) Interaction of surfactin, a biosurfactant from *Bacillus subtilis*, with inorganic cations. *Biotechnol Lett* 14:713–718
- Tiberg F, Brinck J, Grant L (2000) Adsorption and surface-induced self-assembly of surfactants at the solid-aqueous interface. *Curr Opin Colloid Interface Sci* 4:411–419
- Zou A-H, Liu J, Mu B-Z (2010) Interaction between the natural lipopeptide [Glu1, Asp5] surfactin-C15 and hemoglobin: a spectroscopic and electrochemical investigation. *Colloid Surf A* 369:154–159